Electronic Supplementary Material (ESI) for Organic Chemistry Frontiers.

Supporting Information

I. Materials and Methods

All manipulations were carried out using break-and-seal[1] and glovebox techniques under an atmosphere of argon. Tetrahydrofuran (THF) and hexanes (Sigma-Aldrich) were dried over Na/benzophenone and distilled prior to use. THF-d_8 (≥99.5 atom %D, Sigma-Aldrich) was dried over NaK_2 alloy and vacuum-transferred. Twistacene **1** was prepared according to a procedure reported earlier[2] and used without further purification. Lithium (99.9%), cesium (99.95%), and 18-crown-6 ether (99%) were purchased from Sigma-Aldrich and used as received. The UV-vis absorption spectra were recorded on a Shimadzu 2600i UV-visible Spectrophotometer. The ^{1}H and ^{7}Li NMR spectra were measured using a Bruker Ascend-500 spectrometer (500 MHz for ^{1}H and 126 MHz for ^{7}Li) and referenced to the resonances of THF-d_8. The low-temperature NMR experiment was controlled by a Cryo Diffusion cryogenic tank probe, and liquid N_2 was used as a cooling source. The extreme air- and moisture sensitivity of crystals **2**–**4**, along with the presence of interstitial THF molecules, prevented obtaining elemental analysis data.

[Cs^+(18-crown-6)$_2$][(1^{1-})]·2THF (2·2THF): THF (1.0 mL) was added to a custom-built glass system containing **1** (3.0 mg, 0.003 mmol), excess Cs metal (5.0 mg, 0.038 mmol) and 18-crown-6 (4.0 mg, 0.015 mmol). The mixture was allowed to stir under argon at 25 °C for 10 minutes in a closed system. The initial red color of the suspension quickly changed to purple after 3 minutes. The suspension was filtered, and the bright purple filtrate was layered with 1.5 mL of hexanes. The ampule was sealed and kept at 5 °C. Purple plate crystals were deposited after 7 days. Yield: 2 mg, 70 %. UV-Vis (THF): λ_{max} 506 nm.

[{Li^+(THF_2)}$_2$($C_{74}H_{42}^{2-}$)]·3THF (3·3THF): THF (0.7 mL) was added to a custom-built glass system containing **1** (3.0 mg, 0.003 mmol) and excess Li metal (0.5 mg, 0.070 mmol). The mixture was allowed to stir under argon at 25 °C for 7 hours in a closed system. The initial color of the suspension was red (neutral ligand), and it changed to purple after 15 minutes and deepened to brown-black after 30 minutes. The suspension was filtered, and the black filtrate was layered with 1.0 mL of hexanes. The ampule was sealed and kept at 5 °C. A few dark block-shaped crystals were deposited after 14 days. Yield: *ca*. 20-25 %. ^{1}H NMR (THF-d_8, ppm, 25 °C): δ = 7.95–7.99 (2H, $C_{74}H_{42}^{2-}$), 7.90–7.94 (2H, $C_{74}H_{42}^{2-}$), 7.86–7.89 (2H, $C_{74}H_{42}^{2-}$), 7.84–7.86 (2H, $C_{74}H_{42}^{2-}$),

7.80–7.84 (2H, $C_{74}H_{42}^{2-}$), 7.53–7.57 (2H, $C_{74}H_{42}^{2-}$), 7.13–7.18 (2H, $C_{74}H_{42}^{2-}$), 6.85–6.88 (2H, $C_{74}H_{42}^{2-}$), 6.41–6.48 (8H, $C_{74}H_{42}^{2-}$), 6.34–6.39 (8H, $C_{74}H_{42}^{2-}$), 6.27–6.33 (4H, $C_{74}H_{42}^{2-}$), 6.07–6.11 (2H, $C_{74}H_{42}^{2-}$), 5.85–5.90 (2H, $C_{74}H_{42}^{2-}$), 5.73–5.77 (2H, $C_{74}H_{42}^{2-}$), ^{7}Li (THF-d_8, ppm, 0 °C): δ=−1.13, UV-Vis (THF): λ_{max} 320, 463 nm.

$[Li^{+}(THF)_4]_2[\{Li^{+}(THF)_2\}_2(C_{74}H_{42}^{4-})]\cdot 0.5THF$ (4·0.5THF): THF (0.7 mL) was added to a custom-built glass system containing **1** (3.0 mg, 0.003 mmol) and excess Li metal (0.5 mg, 0.070 mmol). The mixture was allowed to stir under argon at 25 °C for 24 hours in a closed system. The initial color of the suspension was red (neutral ligand), and it changed to purple after 15 minutes and deepened to brown-black after 30 minutes. For the last hour, the mixture was ultrasonicated. The suspension was filtered, and the black filtrate was layered with 1.0 mL of hexanes. The ampule was sealed and kept at 25 °C with a slight temperature gradient. Black blocks were deposited after 14 days. Yield: 1.2 mg, 40 %. UV-Vis (THF): λ_{max} 310, 480 nm.

Note: crystals of **4** have very limited solubility thwarting solution characterization.

II. UV-Vis Spectroscopic Investigation

Sample preparation: THF (3 mL) was added to a glass ampule (O.D. 12 mm) containing **1** (0.2 mg, 0.0002 mmol), excess Li or Cs (1.0 mg, 0.008-0.14 mmol), w/o 2 eq. of 18-crown-6 ether. The ampule was sealed under argon, and UV-Vis absorption spectra were monitored at different reaction times (total 24 hours) at 25 °C.

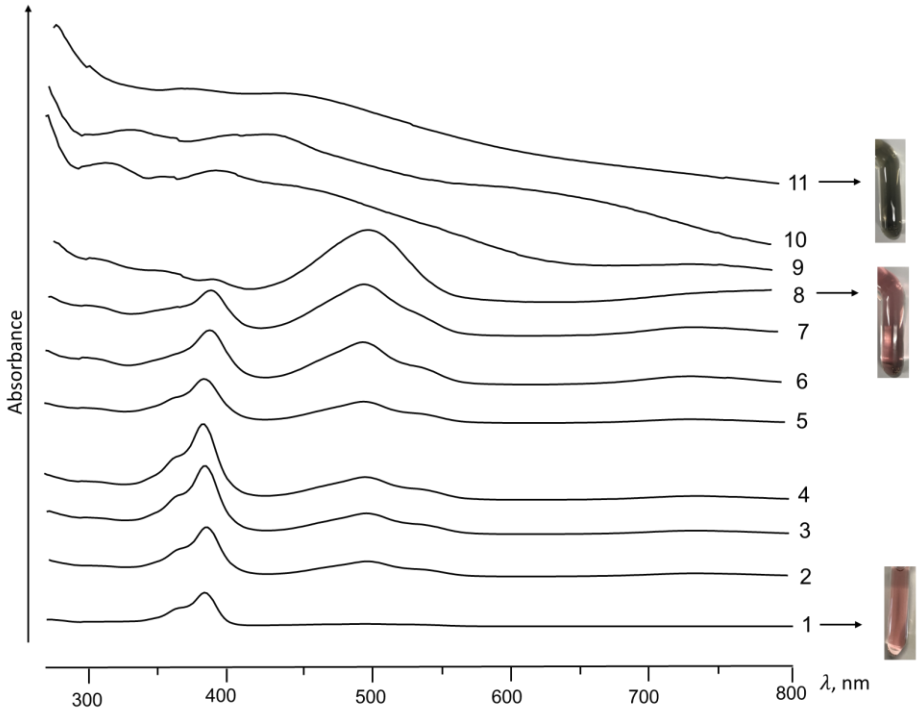

Label	Time (min)
1	1
2	2
3	3
4	4
5	5
6	6
7	9
8	10
9	15
10	60
11	1440

Figure S1. UV-Vis spectra of Cs/18-crown-6/**1** in THF.

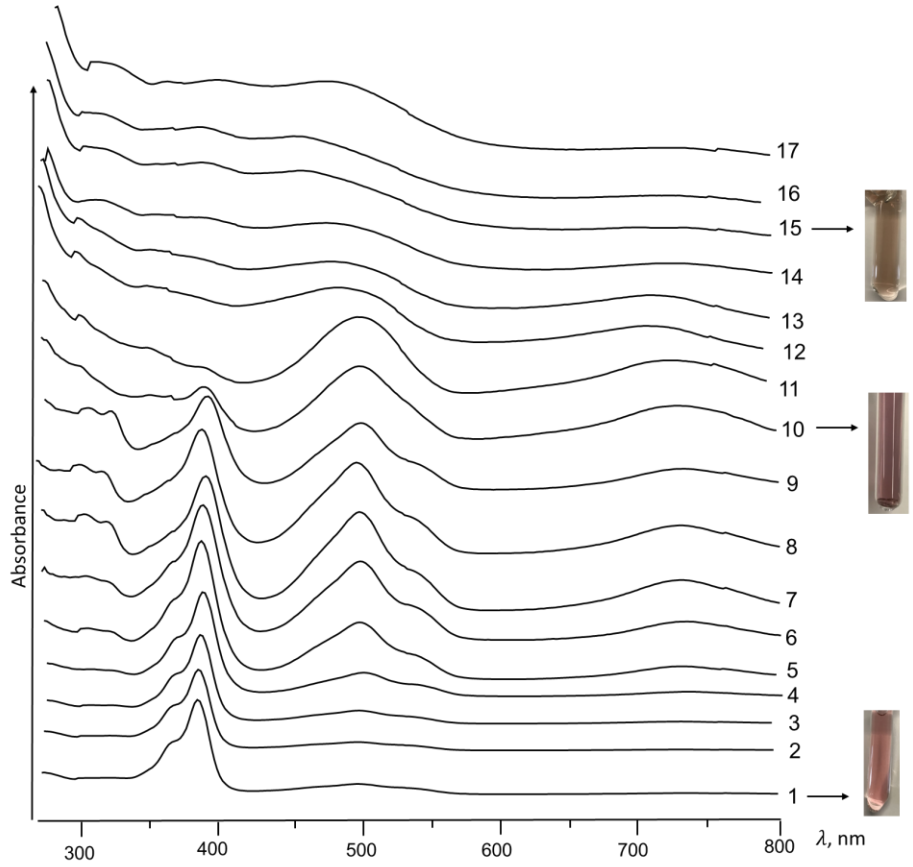

Label	Time (min)
1	1
2	2
3	8
4	10
5	15
6	25
7	30
8	35
9	45
10	55
11	65
12	75
13	85
14	105
15	205
16	305
17	1440

Figure S2. UV-Vis spectra of Li/**1** in THF.

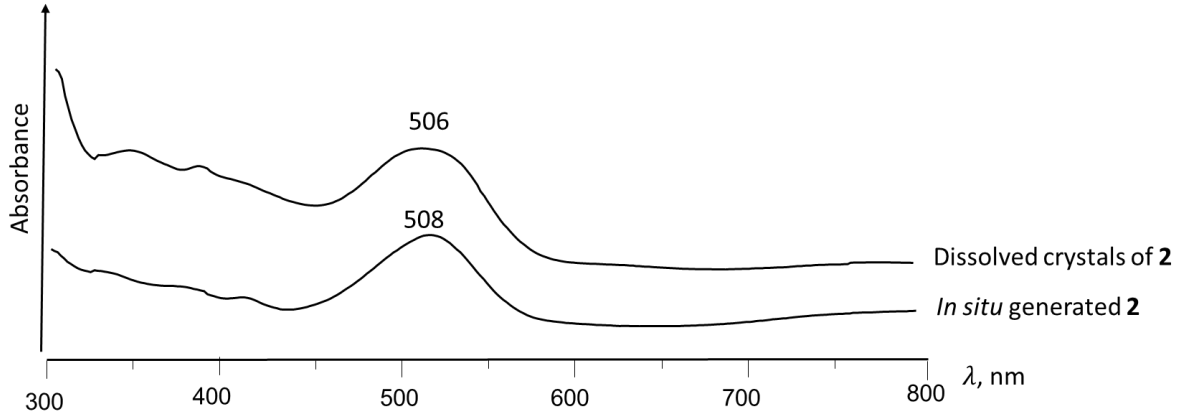

Figure S3. UV-Vis spectra of crystals of **2** dissolved and *in situ* generated **2** in THF.

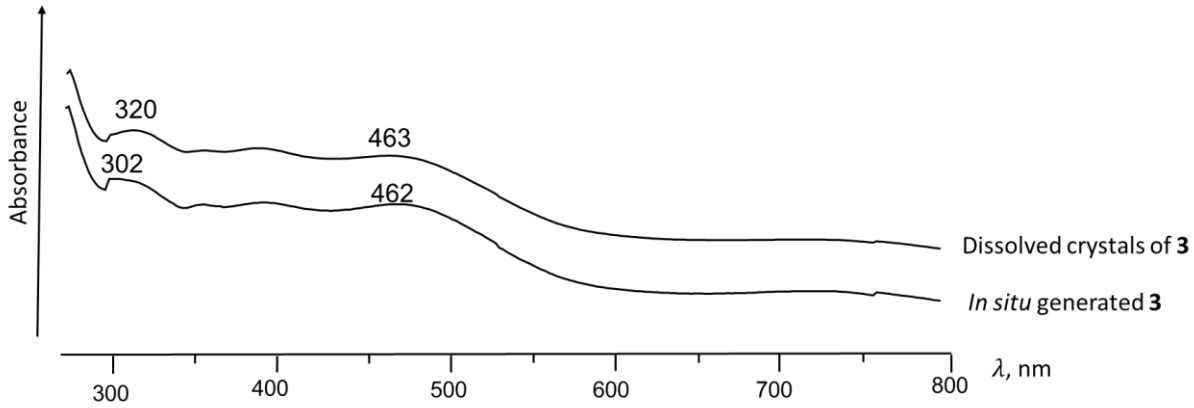

Figure S4. UV-Vis spectra of crystals of **3** dissolved and *in situ* generated **3** in THF.

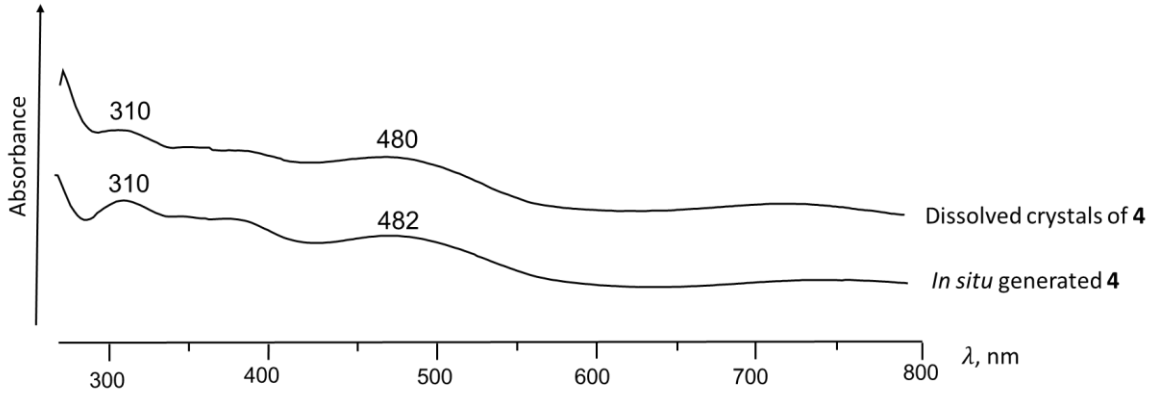

Figure S5. UV-Vis spectra of crystals of **4** dissolved and *in situ* generated **4** in THF.

III. NMR Spectroscopic Investigation

Sample preparation: **1** (2 mg) was dissolved in THF-d_8 (0.7 mL) in an NMR tube that was sealed under argon.

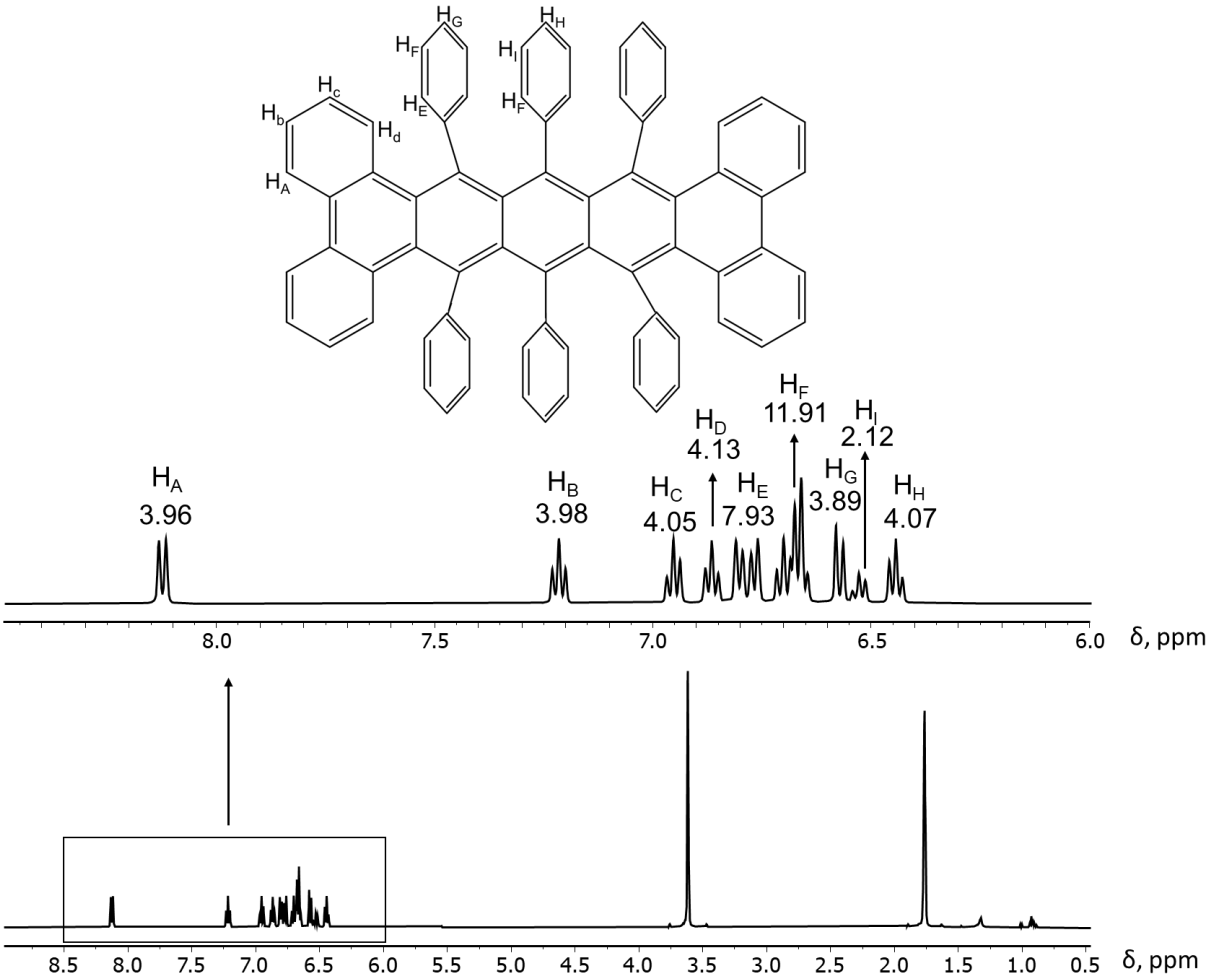

Figure S6. ^{1}H NMR spectrum of **1** in THF-d_8 at 25 °C with integrations and peak assignment.

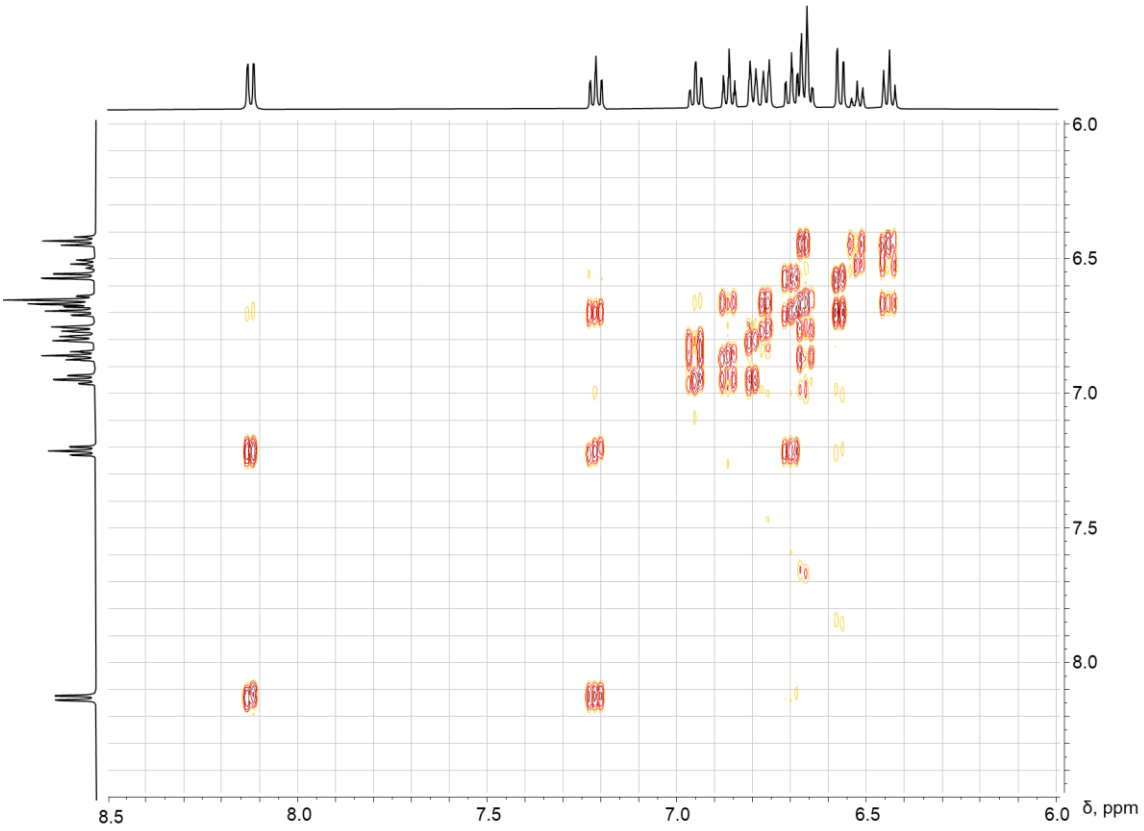

Figure S7. ^{1}H-^{1}H COSY NMR of **1** in THF-d_8, aromatic region.

Sample preparation: **1** (2 mg) and Li metal (0.5 mg, 0.070 mmol) were added to an NMR tube containing THF-d_8 (0.7 mL) that was sealed under argon. The NMR spectra were monitored at different reaction times during ultrasonication (total 70 min).

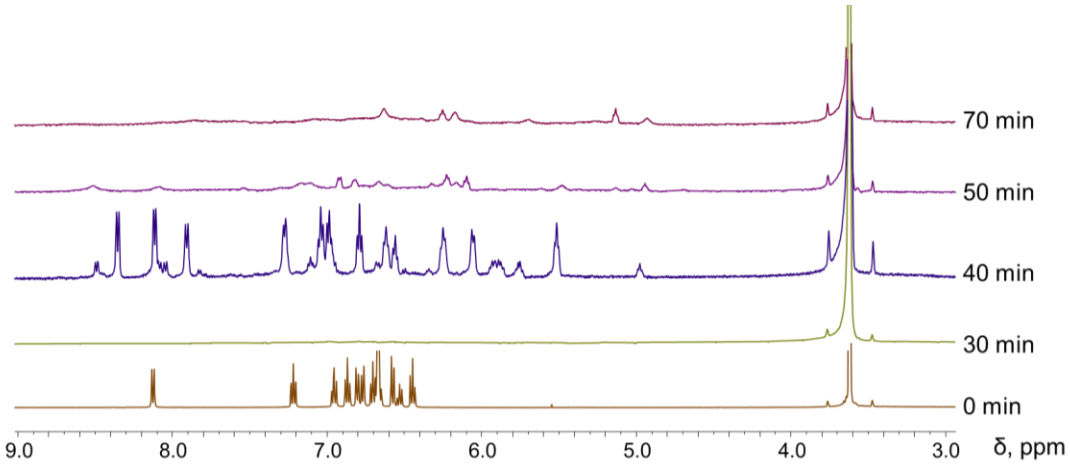

Figure S8. ^{1}H NMR spectra of *in situ* Li/**1** in THF-d_8, aromatic region.

Sample preparation: Crystals of **3** and **4** (2 mg) were washed several times with hexanes and dried *in-vacuo*. Crystals were dissolved in THF-d_8 (0.7 mL) in an NMR tube that was sealed under argon.

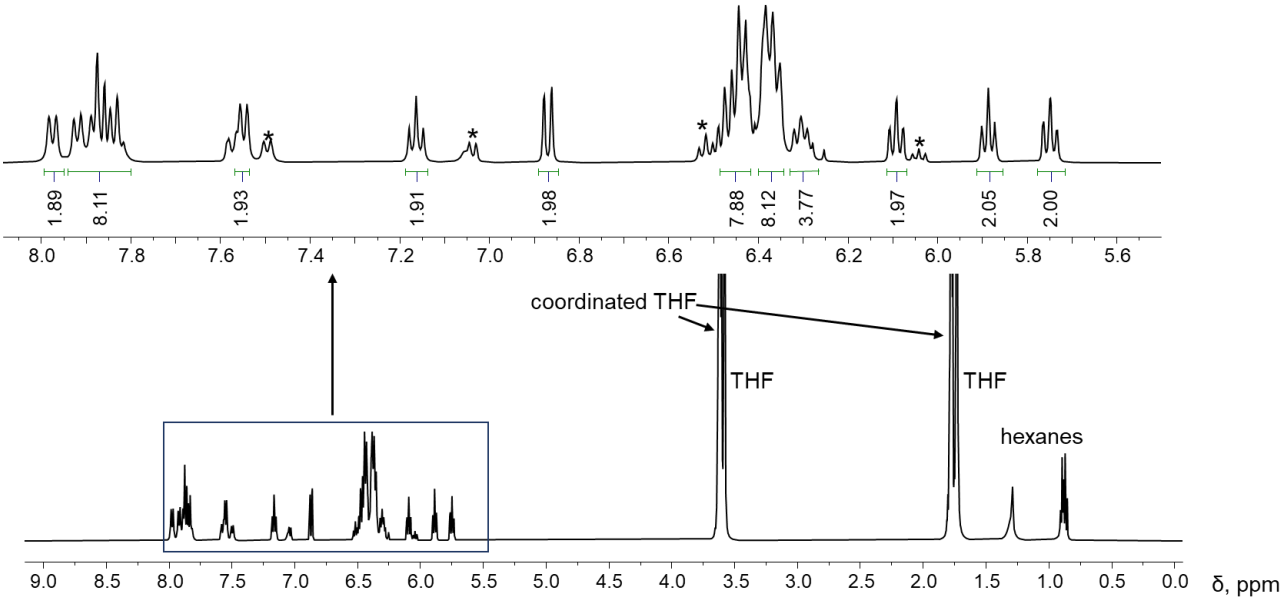

Figure S9. ^{1}H NMR spectrum of **3** in THF-d_8 at 25 °C with integration.

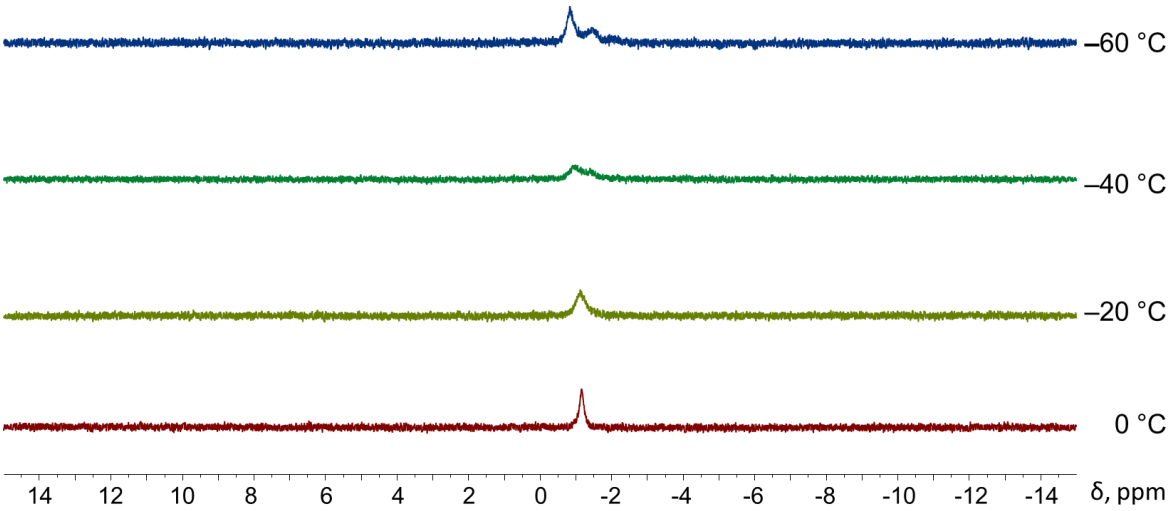

Figure S10. Variable temperature ^{7}Li NMR spectra of **3** in THF-d_8.

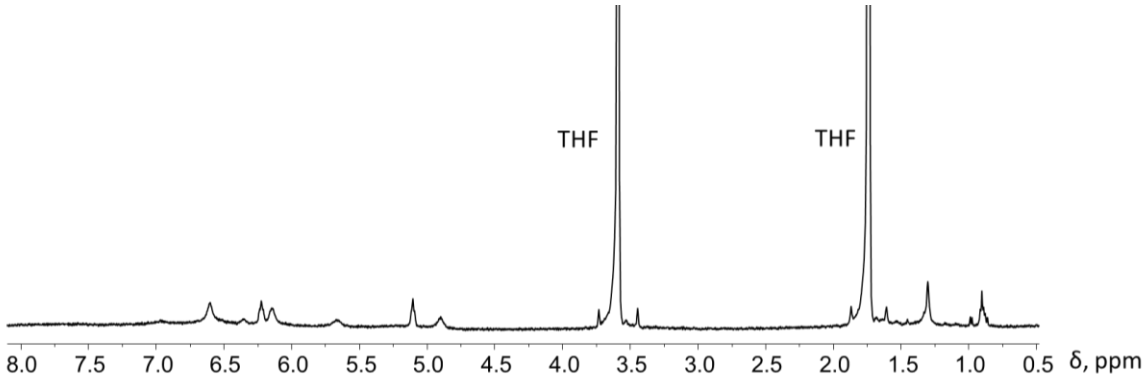

Figure S11. ^{1}H NMR spectrum of **4** in THF-d_8 at 25 °C.

*Note: Crystals of **4** have very low solubility.*

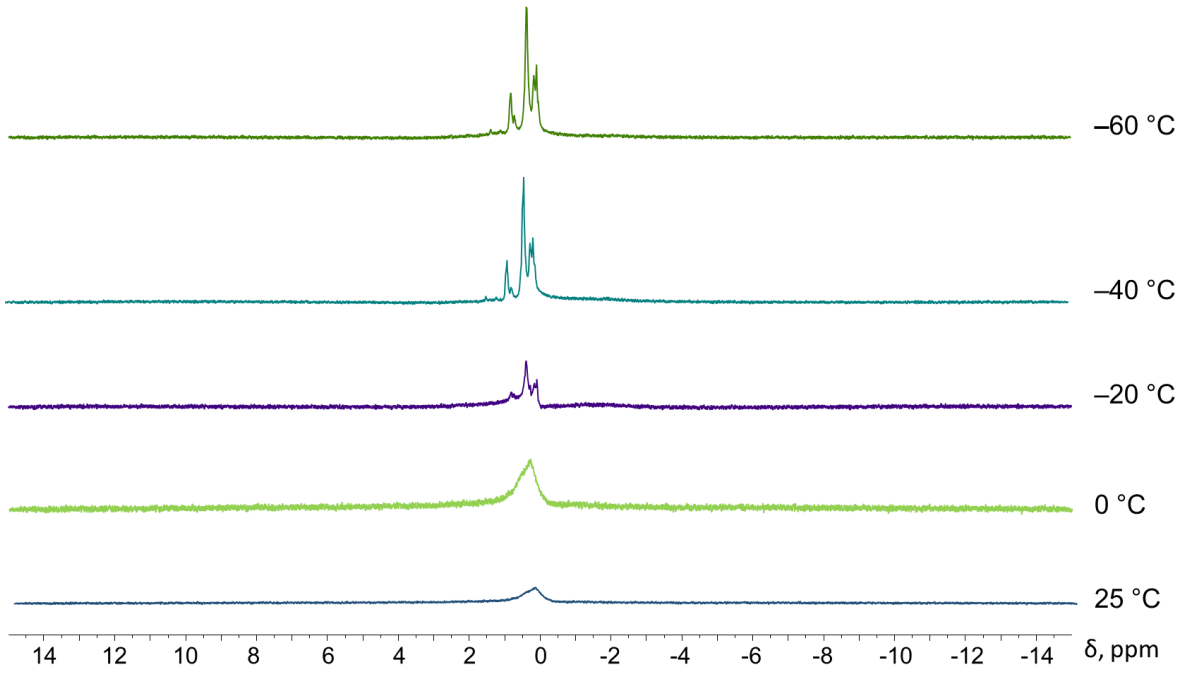

Figure S12. Variable temperature ^{7}Li NMR spectra of **4** in THF-d_8.

IV. EPR Spectroscopic Investigation

Sample preparation: Crystals of **2** were moved into the glovebox and the off-white solution was removed. The crystalline material (0.5 mg) was dried *in-vacuo* and loaded into a quartz capillary tube (O.D. 1.25 mm). The tube was sealed under argon and EPR spectrum was collected at 30.6 °C on a LINEV ADANI Spinscan X Electron Paramagnetic Resonance Spectrometer.

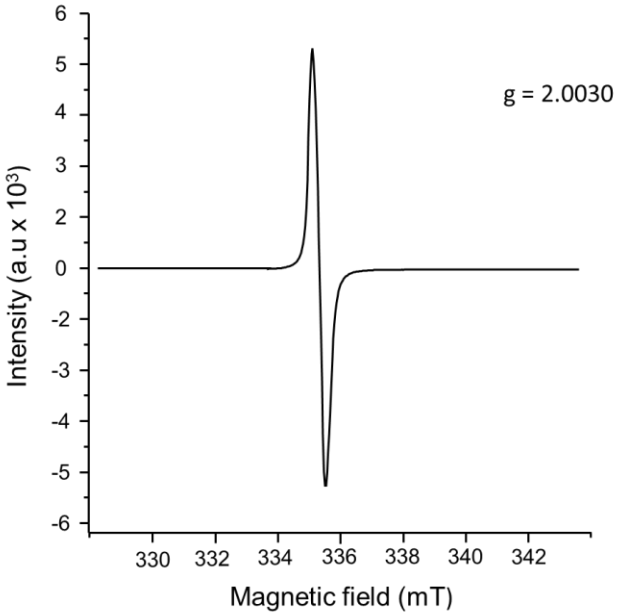

Figure S13. EPR spectrum of **2**, collected at 30.6 °C.

V. Crystal Structure Solution and Refinement

Data collection of **3** was performed on a Bruker D8 VENTURE single crystal X-ray diffractometer equipped with a PHOTON 100 CMOS detector and a Mo-target X-ray tube (λ = 0.71073 Å) at 100(2) K. Data were collected at 50 kV and 30 mA with an appropriate 0.5° ω scan strategy. Data collections of **2** and **4** were performed at 100(2) K on a Huber Kappa 4-circle system with a DECTRIS PILATUS3 X 2M(CdTe) pixel array detector using ϕ scans located at the Advanced Photon Source, Argonne National Laboratory (NSF's ChemMatCARS, Sector 15, Beamline 15-ID-D). Data reduction and integration were performed with the Bruker software package SAINT (version 8.38A).[3] Data were corrected for absorption effects using the empirical methods as implemented in SADABS (version 2016/2).[4] The structures were solved by SHELXT (version 2018/2)[5] and refined by full-matrix least-squares procedures using the Bruker SHELXTL (version 2019/2)[6] software package through the OLEX2 graphical interface.[7] All non-hydrogen atoms, including those in disordered parts, were refined anisotropically. Hydrogen atoms were included in idealized positions for structure factor calculations with U_{iso}(H) = 1.2 U_{eq}(C). In **2**, one 18-crown-6 molecule was found to be disordered. In **3**, four THF molecules and part of the dianion core were found to be disordered. In **4**, eight THF molecules were found to be disordered. The disordered molecules and groups were modeled with two orientations with their relative occupancies refined. The geometries of the disordered parts were restrained to be similar. The anisotropic displacement parameters of the disordered molecules were restrained to have the same U_{ij} components, with a standard uncertainty of 0.01 Å^2. In each unit cell of **3**, twenty-four THF solvent molecules were found to be severely disordered and removed by the Olex2's solvent mask subroutine.[7] The total void volume was 9161.9 Å^3, equivalent to 43.75 % of the unit cell's total volume. In each unit cell of **4**, two THF solvent molecules were found to be severely disordered and removed by the Olex2's solvent mask subroutine.[7] The total void volume was 497.4 Å^3, equivalent to 4.87 % of the unit cell's total volume. Further crystal and data collection details are listed in Table S1.

.

Table S1. Crystal data and structure refinement parameters for **2**, **3**, and **4**.

Compound	**2**	**3**	**4**
Empirical formula	$C_{106}H_{110}CsO_{14}$	$C_{102}H_{98}Li_2O_7$	$C_{124}H_{142}Li_4O_{12.5}$
Formula weight	1740.84	1449.68	1860.13
Temperature (K)	100(2)	100(2)	100(2)
Wavelength (Å)	0.41329	0.71073	0.41328
Crystal system	Monoclinic	Tetragonal	Monoclinic
Space group	$P2_1/c$	$P4_2/n$	$P2_1/n$
a (Å)	18.3668(6)	26.022(3)	17.3967(10)
b (Å)	17.8645(5)	26.022(3)	32.0271(18)
c (Å)	26.8298(8)	30.925(4)	18.3476(10)
α (°)	90.00	90.00	90.00
β (°)	98.8420(10)	90.00	92.3510(10)
γ (°)	90.00	90.00	90.00
V (Å^3)	8698.6(5)	20941(5)	10214.1(10)
Z	4	8	4
ρ_{calcd} (g·cm^{-3})	1.329	0.920	1.210
μ (mm^{-1})	0.131	0.056	0.033
F(000)	3652	6176	3992
Crystal size (mm)	0.11×0.12×0.14	0.11×0.32×0.44	0.04×0.09×0.13
θ range for data collection (°)	0.893-21.955	2.748-25.105	0.991-15.287
Reflections collected	315713	468904	113482
Independent reflections	44246 [R_{int} = 0.0466]	18583 [R_{int} = 0.1361]	22121 [R_{int} = 0.0762]
Transmission factors (min/max)	0.6466/0.6715	0.6143/0.6659	0.5832/0.7439
Data/restraints/params.	44246/598/1254	18583/3378/1367	22121/1282/1607
$R1$,[a] $wR2$[b] ($I > 2\sigma(I)$)	0.0256, 0.0759	0.1043, 0.2893	0.0578, 0.1651
$R1$,[a] $wR2$[b] (all data)	0.0266, 0.0766	0.1480, 0.3268	0.0793, 0.1836
Quality-of-fit[c]	1.031	1.043	1.126

$R_{int} = \Sigma|F_o^2 - \langle F_o^2 \rangle|/\Sigma|F_o^2|$

[a]$R1 = \Sigma||F_o|-|F_c||/\Sigma|F_o|$. [b]$wR2 = [\Sigma[w(F_o^2-F_c^2)^2]/\Sigma[w(F_o^2)^2]]$.

[c]Quality-of-fit = $[\Sigma[w(F_o^2-F_c^2)^2]/(N_{obs}-N_{params})]^{½}$, based on all data.

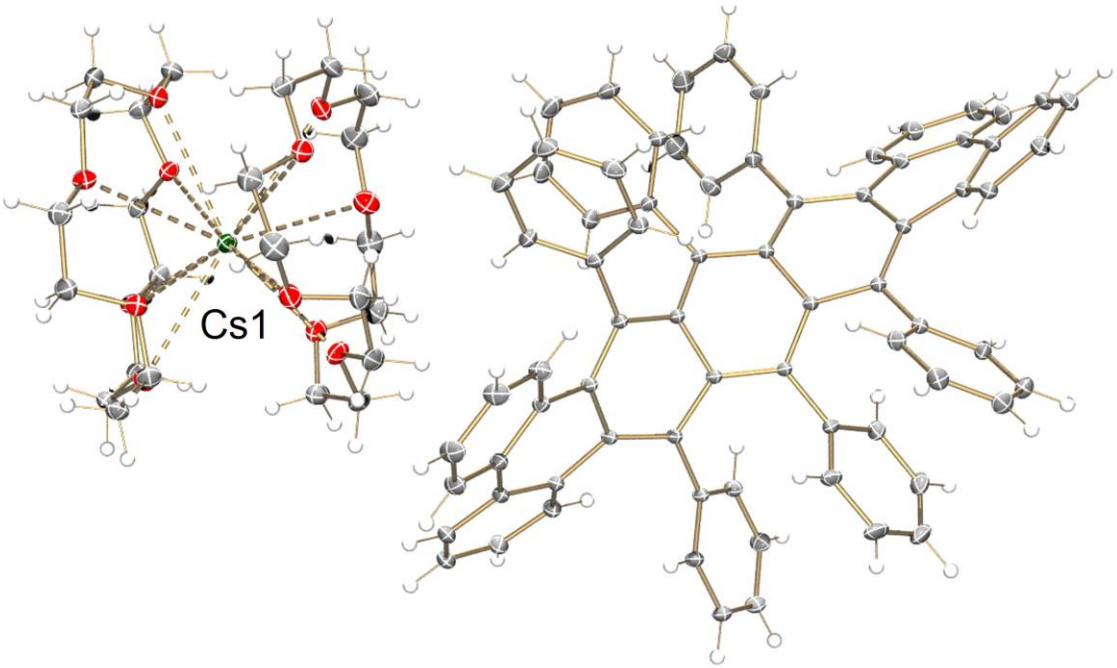

Figure S14. ORTEP diagram of the asymmetric unit of **2** with thermal ellipsoids at 50% probability level. The color scheme used: C grey, H white, O red, Cs green.

Table S2. C–H···π interactions (Å) in **2** along with labeling scheme.

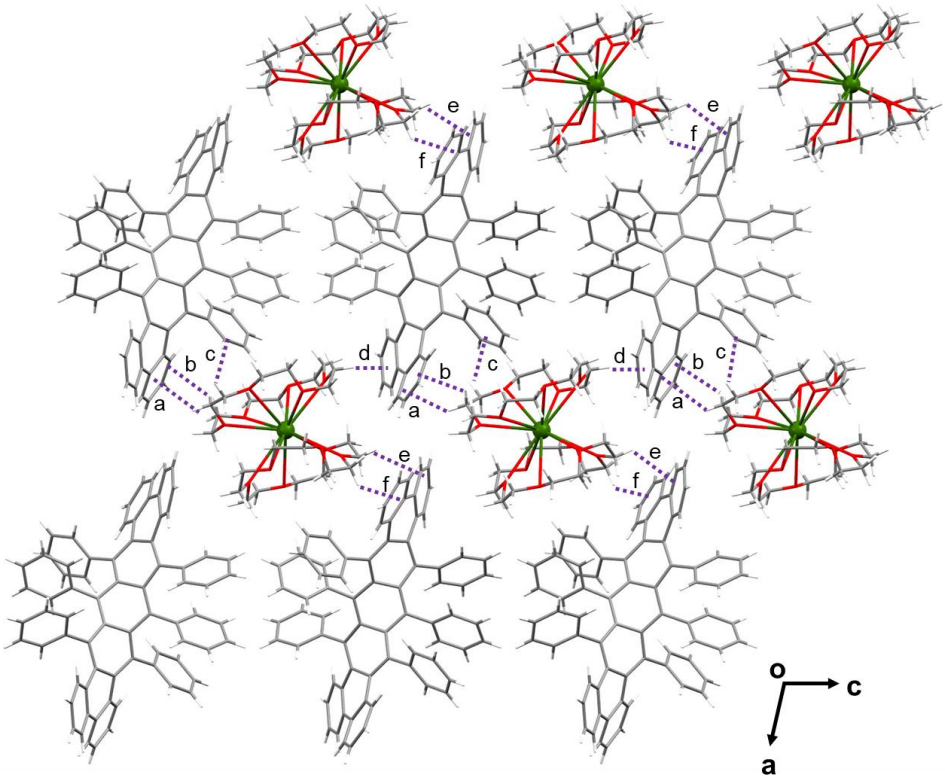

C–H···π interaction	Distance
a	2.787(3)
b	2.576(2)
c	2.103(2)
d	2.694(3)
e	2.677(2)
f	2.704(2)

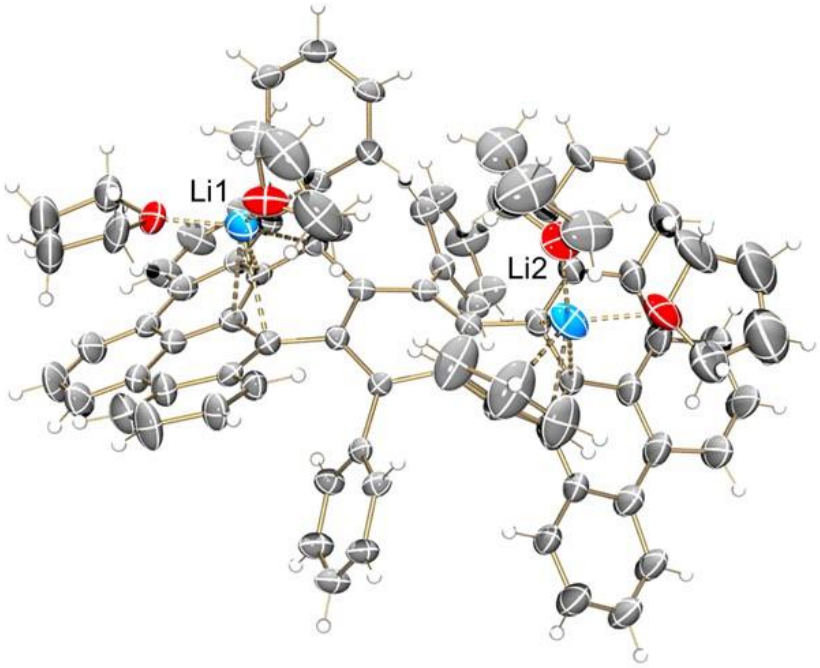

Figure S15. ORTEP diagram of the asymmetric unit of **3** with thermal ellipsoids at 50% probability level. The color scheme used: C grey, H white, O red, Li slate blue.

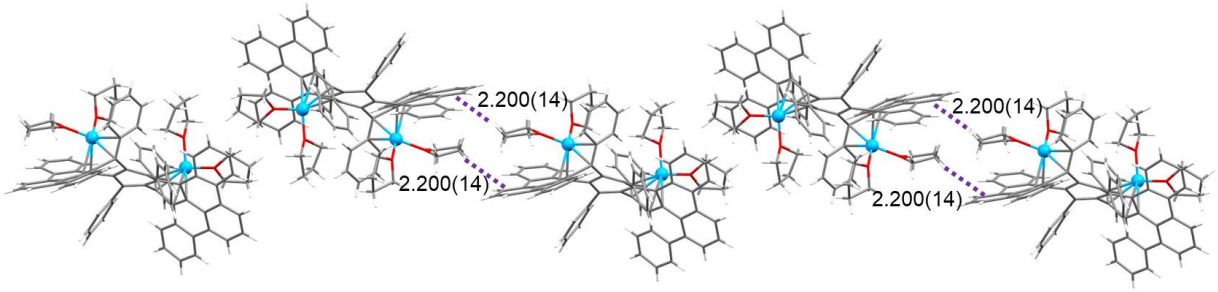

Figure S16. C–H···π interactions (Å) in **3**, mixed model.

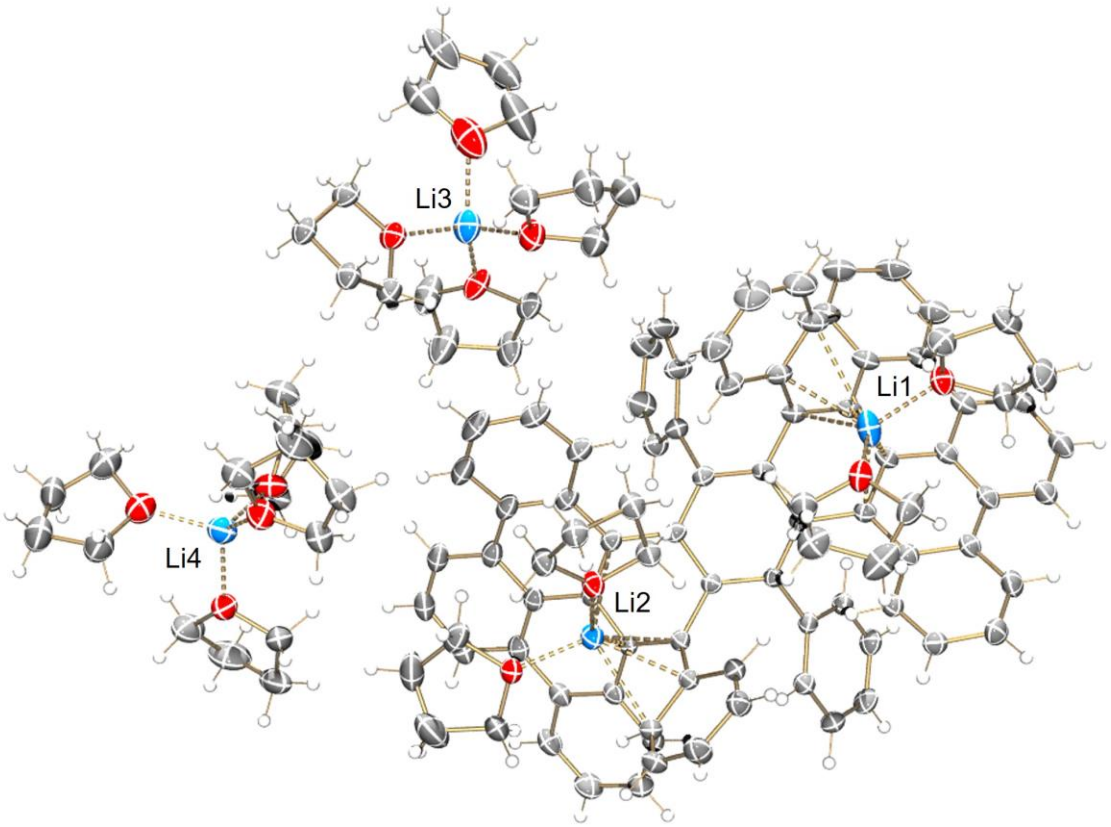

Figure S17. ORTEP diagram of the asymmetric unit of **4** with thermal ellipsoids at 50% probability level. The color scheme used: C grey, H white, O red, Li slate blue.

Table S3. C–H···π interactions (Å) in **4** along with labeling scheme. Two different views are shown.

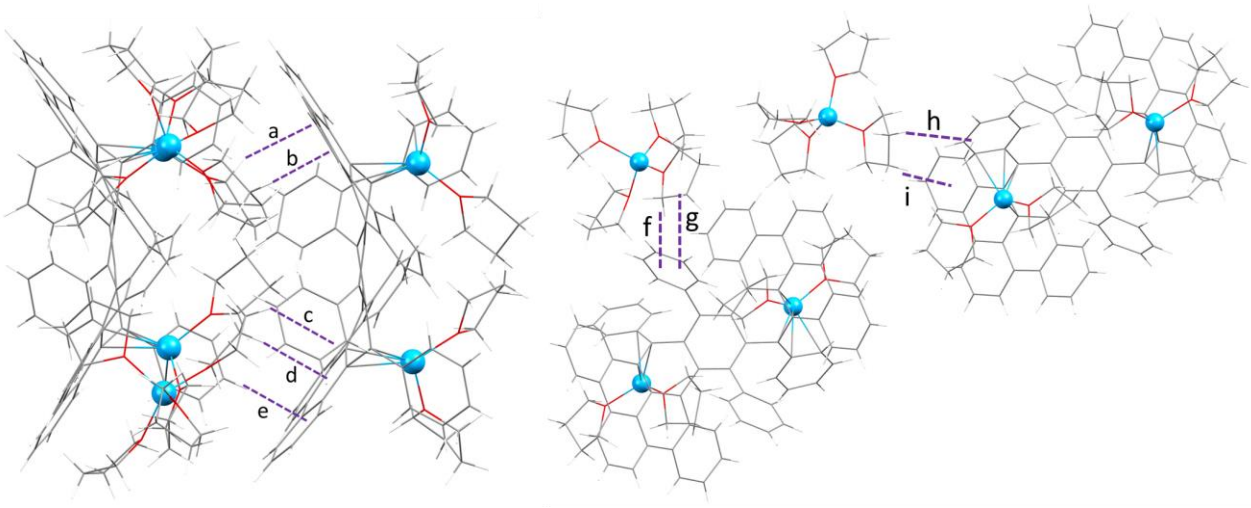

C–H···π interaction	Distance	C–H···π interaction	Distance
a	2.484(4)	f	2.558(6)
b	2.509(5)	g	2.655(7)
c	2.554(6)	h	2.456(5)
d	2.651(5)	i	2.791(5)
e	2.739(5)		

Table S4. Li–C distances (Å) in **3**, along with a labeling scheme.

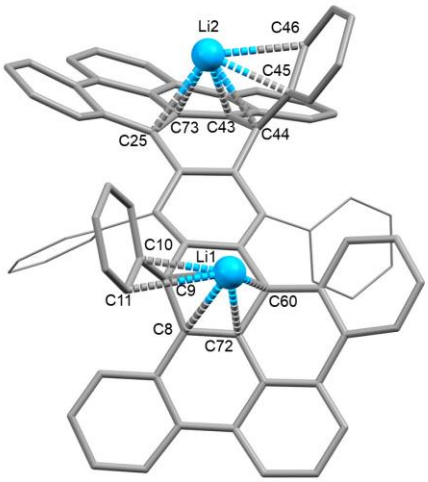

Bond	Distance	Bond	Distance
Li1–C8	2.575(8)	Li2–C25	2.542(8)
Li1–C9	2.360(8)	Li2–C43	2.508(8)
Li1–C10	2.408(9)	Li2–C44	2.386(8)
Li1–C60	2.402(9)	Li2–C45	2.366(8)
Li1–C11	2.819(8)	Li2–C46	2.622(9)
Li1–C72	2.481(8)	Li2–C73	2.469(9)

Table S5. Li–C distances (Å) in **4**, along with a labeling scheme.

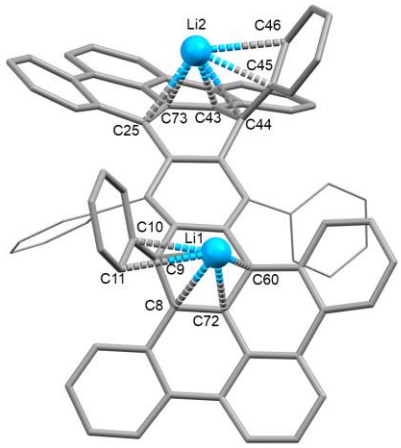

Bond	Distance	Bond	Distance
Li1–C8	2.439(4)	Li2–C25	2.820(4)
Li1–C9	2.360(8)	Li2–C43	2.434(3)
Li1–C10	2.415(4)	Li2–C44	2.441(3)
Li1–C11	2.714(4)	Li2–C45	2.391(3)
Li1–C60	2.571(4)	Li2–C46	2.462(3)
Li1–C72	2.424(4)	Li2–C73	2.504(3)

Table S6. Selected C–C bond length distances (Å) in **2**.

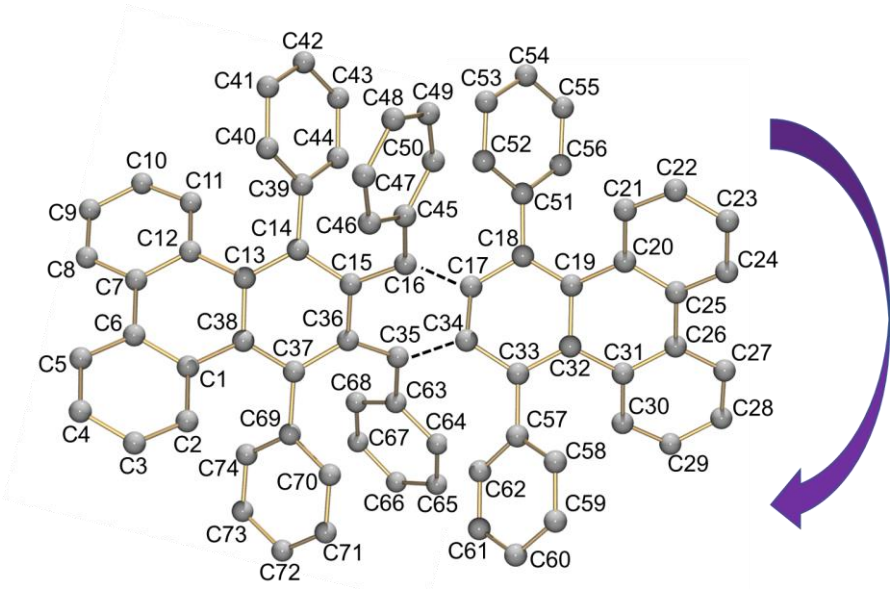

Bond	Distance	Bond	Distance	Bond	Distance
C1–C2	1.4154(9)	C23–C24	1.3847(9)	C48–C49	1.3924(13)
C1–C6	1.4181(8)	C24–C25	1.4075(8)	C49–C50	1.3931(9)
C1–C38	1.4748(8)	C25–C26	1.4599(8)	C50–C45	1.3992(8)
C2–C3	1.3899(9)	C25–C20	1.4203(8)	C51–C52	1.4027(8)
C3–C4	1.3899(9)	C26–C27	1.4101(8)	C52–C53	1.3948(8)
C4–C5	1.3850(10)	C26–C31	1.4193(8)	C53–C54	1.3936(9)
C5–C6	1.4108(8)	C27–C28	1.3844(10)	C54–C55	1.3933(9)
C6–C7	1.4587(9)	C28–C29	1.3997(10)	C55–C56	1.3940(8)
C7–C8	1.4109(8)	C29–C30	1.3864(9)	C56–C51	1.4063(8)
C7–C12	1.4204(8)	C30–C31	1.4164(8)	C57–C58	1.3978(8)
C8–C9	1.3844(10)	C31–C32	1.4686(8)	C58–C59	1.3956(9)
C9–C10	1.4032(10)	C32–C33	1.4083(8)	C59–C60	1.3934(11)
C10–C11	1.3888(8)	C33–C34	1.4294(7)	C60–C61	1.3902(11)
C11–C12	1.4170(9)	C33–C57	1.4917(8)	C61–C62	1.3937(9)
C12–C13	1.4694(8)	C34–C35	1.4272(7)	C62–C57	1.4026(8)
C13–C14	1.4084(7)	C35–C36	1.4198(8)	C63–C35	1.4836(8)
C13–C38	1.4417(8)	C36–C37	1.4401(7)	C63–C64	1.4013(8)
C14–C15	1.4302(7)	C37–C38	1.4076(8)	C64–C65	1.3935(9)
C15–C16	1.4335(7)	C37–C69	1.4864(8)	C65–C66	1.3964(11)

C15–C36	1.4504(8)	C39–C14	1.4888(8)	C66–C67	1.3891(11)
C16–C17	1.4220(7)	C39–C40	1.4007(8)	C67–C68	1.3910(9)
C17–C18	1.4453(7)	C40–C41	1.3920(8)	C68–C63	1.3985(8)
C17–C34	1.4488(7)	C41–C42	1.3938(9)	C69–C70	1.3979(8)
C18–C19	1.4096(7)	C42–C43	1.3957(9)	C70–C71	1.3923(10)
C18–C51	1.4855(7)	C43–C44	1.3938(9)	C71–C72	1.3939(12)
C19–C20	1.4702(8)	C44–C39	1.4009(8)	C72–C73	1.3924(11)
C19–C32	1.4366(7)	C45–C16	1.4832(8)	C73–C74	1.3927(9)
C20–C21	1.4147(8)	C45–C46	1.4020(8)	C74–C69	1.4028(8)
C21–C22	1.3874(8)	C46–C47	1.3936(9)		
C22–C23	1.4026(9)	C47–C48	1.3910(13)		

Table S7. Selected C–C bond length distances (Å) in **3** and **4**.

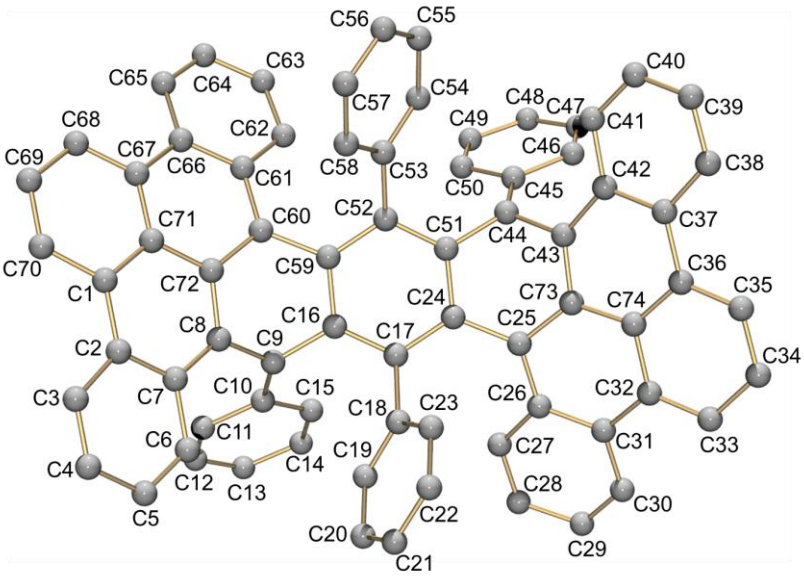

Bond	3	4	Bond	3	4
C1–C2	1.447(6)	1.447(3)	C35–C36	1.366(9)	1.413(2)
C1–C70	1.442(11)	1.407(3)	C36–C37	1.455(11)	1.448(2)
C1–C71	1.428(6)	1.435(2)	C36–C74	1.405(10)	1.428(2)
C2–C7	1.414(6)	1.432(3)	C37–C38	1.427(10)	1.407(2)
C2–C3	1.450(11)	1.411(2)	C37–C42	1.432(10)	1.438(2)
C3–C4	1.345(9)	1.378(3)	C38–C39	1.351(13)	1.374(3)
C4–C5	1.429(9)	1.402(3)	C39–C40	1.364(12)	1.404(3)
C5–C6	1.361(10)	1.370(3)	C40–C41	1.377(9)	1.368(2)
C7–C8	1.410(5)	1.428(2)	C41–C42	1.404(10)	1.428(2)
C7–C6	1.442(18)	1.423(3)	C42–C43	1.468(11)	1.418(2)
C8–C9	1.464(5)	1.472(2)	C43–C44	1.476(5)	1.482(2)
C9–C10	1.431(5)	1.420(2)	C43–C73	1.398(5)	1.413(2)
C8–C72	1.404(5)	1.414(2)	C44–C45	1.404(5)	1.410(2)
C9–C16	1.473(5)	1.484(2)	C44–C51	1.483(5)	1.484(2)
C10–C11	1.429(6)	1.442(2)	C45–C46	1.436(5)	1.442(2)
C10–C15	1.429(6)	1.431(3)	C45–C50	1.445(5)	1.445(2)
C11–C12	1.385(7)	1.385(3)	C46–C47	1.375(5)	1.383(2)
C12–C13	1.363(8)	1.377(4)	C47–C48	1.375(6)	1.392(3)
C13–C14	1.394(7)	1.395(3)	C48–C49	1.392(6)	1.405(3)

C14–C15	1.370(6)	1.375(3)	C49–C50	1.358(5)	1.367(2)
C16–C17	1.401(5)	1.419(2)	C51–C52	1.414(5)	1.423(2)
C16–C59	1.431(5)	1.422(2)	C52–C53	1.487(5)	1.486(2)
C17–C18	1.494(8)	1.495(2)	C52–C59	1.416(5)	1.429(2)
C17–C24	1.430(5)	1.427(2)	C53–C54	1.407(5)	1.403(2)
C18–C19	1.393(8)	1.400(2)	C53–C58	1.391(5)	1.404(2)
C18–C23	1.367(8)	1.402(2)	C54–C55	1.388(6)	1.396(2)
C19–C20	1.406(8)	1.393(3)	C55–C56	1.397(6)	1.384(3)
C20–C21	1.379(10)	1.370(3)	C56–C57	1.387(7)	1.388(3)
C21–C22	1.361(10)	1.389(3)	C57–C58	1.365(6)	1.382(2)
C22–C23	1.383(9)	1.383(3)	C59–C60	1.488(5)	1.479(2)
C24–C25	1.469(5)	1.477(2)	C60–C61	1.429(5)	1.433(2)
C25–C26	1.394(11)	1.435(2)	C60–C72	1.434(5	1.435(2)
C25–C73	1.436(5)	1.428(2)	C61–C66	1.425(6)	1.431(2)
C24–C51	1.417(5)	1.426(2)	C61–C62	1.435(16)	1.425(2)
C26–C27	1.426(10)	1.422(2)	C66–C67	1.471(6)	1.456(2)
C26–C31	1.441(9)	1.432(2)	C66–C65	1.457(13)	1.407(2)
C27–C28	1.382(9)	1.371(3)	C67–C68	1.381(10)	1.402(2)
C28–C29	1.435(12)	1.400(3)	C67–C71	1.419(6)	1.425(2)
C29–C30	1.337(12)	1.365(3)	C62–C63	1.385(9)	1.369(2)
C30–C31	1.415(11)	1.416(2)	C63–C64	1.375(10)	1.397(2)
C31–C32	1.435(10)	1.451(3)	C64–C65	1.343(11)	1.372(3)
C32–C33	1.385(9)	1.405(2)	C68–C69	1.417(10)	1.390(3)
C32–C74	1.459(10)	1.425(2)	C69–C70	1.365(10)	1.380(3)
C33–C34	1.447(12)	1.380(3)	C71–C72	1.438(5)	1.436(2)
C34–C35	1.390(13)	1.377(3)	C73–C74	1.434(10)	1.447(2)

Table S8. Selected dihedral (green) and torsion (red) angles (°) between the phenyl rings of **1** and **1**$^{1-}$, along with a labeling scheme.

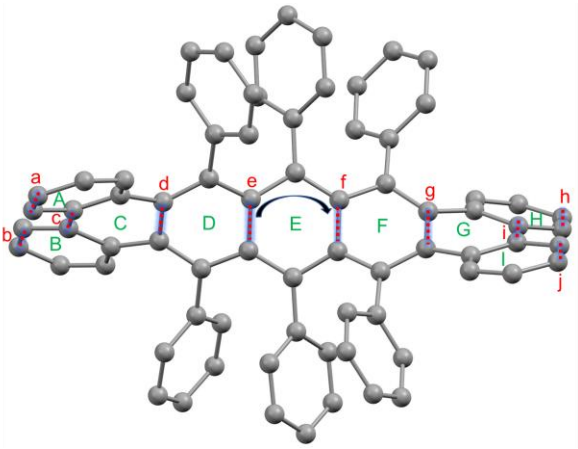

	Angle	1	Cs-**1**$^{1-}$	Angle	1	Cs-**1**$^{1-}$
Dihedral Angle	A-H	41.35	36.49	C-G	59.99	58.26
	A-I	32.65	32.44	C-E	58.75	59.88
	B-H	34.74	33.59	D-F	58.49	59.63
	B-I	42.98	43.41	D-E	29.10	28.06
Torsion Angle	a/h	-146.61	-149.00	c/i	-143.36	-142.12
	a/j	-145.78	-144.54	c/e	-55.50	-55.36
	b/h	-144.43	-146.05	d/g	-85.47	-87.55
	b/j	-143.98	-139.30	e/f	-26.92	-29.90

Table S9. Selected dihedral (green) and torsion (red) angles (°) between phenyl rings of **1** and the $C_{74}H_{42}^{2-}$ core in **3**, along with a labeling scheme.

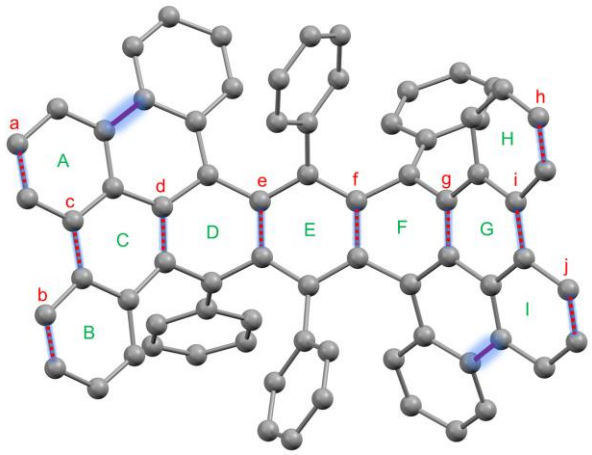

	Angle	1	Li_2-$C_{74}H_{42}^{2-}$ **3**	Li_4-$C_{74}H_{42}^{4-}$ **4**	Angle	1	Li_2-$C_{74}H_{42}^{2-}$ **3**	Li_4-$C_{74}H_{42}^{4-}$ **4**
Dihedral Angle	A-H	41.35	71.83	69.76	C-G	59.99	71.65	65.85
	A-I	32.65	66.26	65.65	C-E	58.75	36.89	36.04
	B-H	34.74	77.59	76.92	D-F	58.49	31.16	27.06
	B-I	42.98	70.87	72.50	D-E	29.10	15.47	15.33
Torsion Angle	a/h	146.61	12.75	-18.44	c/i	143.36	12.30	-18.16
	a/j	145.78	21.86	-22.02	c/e	-55.50	11.51	-13.36
	b/h	144.43	8.80	-16.84	d/g	-85.47	-2.31	-1.22
	b/j	143.98	15.98	-18.82	e/f	-26.92	-4.93	4.86

VI. Computational Details

General Details

All calculations were performed with the ORCA 5.0.3 software package[8] using the PBE0[9,10] functional and the def2-TZVP[11,12] basis set. Dispersion effects were accounted for using Grimme's D3 correction with Becke-Johnson damping.[13,14]

For the naked twistacene structures (**1**, $\mathbf{1}^{\mathbf{1-}}$, $\mathbf{1}^{\mathbf{2-}}$, $\mathbf{1}_{\boldsymbol{mono}}^{\mathbf{2-}}$, $\mathbf{1}_{\boldsymbol{bis}}^{\mathbf{2-}}$, and $\mathbf{1}_{\boldsymbol{bis}}^{\mathbf{4-}}$), full optimizations were performed and frequency calculations confirmed the optimized structures to be real minima (i.e., $N_{imag} = 0$). For the complexes (structures **2**, **3**, and **4**), constrained optimizations were performed, in which only the hydrogen coordinates were optimized on the crystal-structure coordinates of the metal-twistacene complexes; all other atoms were kept frozen. All optimized structures are provided in an accompanying *.xyz* file.

XYZ coordinates for the NICS calculations[15,16] were generated with the AROMA package,[17] using the geometries optimized as described above. Electrostatic potential maps (ESPs) were generated using MultiWFN 3.6[18] and orca_vpot.[19] Input templates for calculations, ESP analysis and visualizations with PyMOL[20] are provided below.

All NICS calculations were performed using the $NICS(1.7)_{ZZ}$ metric[21] and are reported in ppm. For all twistacene molecules, the $NICS(1.7)_{ZZ}$ values were calculated for all rings except the two middle pendant rings, for which the NICS probe could not be placed, due to the interference of the neighboring pendant rings.

All reported charges are Löwdin partial charges. All MO visualizations are plotted on an isosurface value of $\alpha = 0.015$.

Input templates

To allow the reproducibility of our computational results, sample input files for calculations and visualizations with PyMOL are provided below.

Full optimizations of the naked twistacene structures were performed using the following keywords:

```
! PBE0 def2-TZVP D3BJ def2/J DefGrid2 TightOpt
*xyzfile <C> <M> <XYZ>
```

Where <C> is the placeholder for charge, <M> is the placeholder for multiplicity and <XYZ> is the placeholder for the file path of the Cartesian coordinates in XMOL format. The second line is omitted in the following input templates for conciseness.

Frequency calculations were performed with the following keywords:

```
! PBE0 def2-TZVP D3BJ def2/J DefGrid2 Freq
```

Constrained optimizations were performed on the crystal-structure coordinates of the metallic complexes **2**, **3** and **4**, in which the heavy atoms were kept frozen, and the H atoms were allowed to optimize using the following input keywords:

```
! PBE0 def2-TZVP D3BJ def2/J DefGrid2 TightOpt

%geom
optimizeHydrogens true
end
```

AROMA was used to place the molecule in the XY plane and the NICS probe was then generated 1.7 Å above the XY plane. The NICS calculations were then performed with ORCA, using the following keywords, where <coordinates> is a placeholder for XYZ coordinates:

```
! PBE0 def2-TZVP D3BJ def2/J DefGrid2 TightSCF NMR
*xyz 0 1
<coordinates>
H:     -0.00000     0.00000     1.70000 NewGTO S 1 1 1e6 1 end
NewAuxJGTO S 1 1 2e6 1 end
*
```

Visualization

The molecular orbitals were visualized with PyMOL using the following script, where <molecule> and <MO> are placeholders for the names of the molecule and the number of the orbital.

```
#load <molecule>.xyz, mol
#load <MO>.cube, orb

##########
# molecule
##########

show sticks
set stick_h_scale, 1
set_bond stick_radius, 0.15, mol
color gray70, elem C
color white, elem H

#########
# orbital
#########

isosurface orb_pos, orb, 0.015
isosurface orb_neg, orb, -0.015

# colors
set_color neg_col, [0, 204, 204]
set_color pos_col, [255, 179, 26]
color pos_col, orb_pos
color neg_col, orb_neg

#########
# general
#########

# Background
bg_color white
set ray_opaque_background, 0

# Lighting
set ambient, 0.2
set ray_shadows, 1
set spec_reflect, 0.6
set spec_power, 600
set spec_count, 3
set shininess, 70
set reflect, 0.5

# General visuals
set ray_trace_mode, 1
set ray_texture, 2
```

```
set antialias, 3
set fog, 1
set fog_start, 0.4

# save
png <molecule_MO>.png, width=1600, height=1200, dpi=300, ray=1
#quit
```

The ESPs were visualized with the following PyMOL script:

```
#load <molecule>.xyz, mol
#load <molecule_density>.cube, dens_cube
#load <molecule_potential>.cube , pot_cube

##########
# molecule
##########

show sticks, mol
hide lines, mol
set_bond stick_radius, 0.1, mol

# colors
color gray70, (elem C)
color white, (elem H)

#########
# MEP
#########

isosurface dens, dens_cube, 0.005
ramp_new spectrum, pot_cube, [-0.1, -0.05, 0, 0.05, 0.1], [blue,
cyan, green, yellow, red]
#ramp_new spectrum, pot_cube, [-0.2, -0.15, -0.1, -0.05, 0], [blue,
cyan, green, yellow, red]
set transparency, 0.2, dens

#########
# general
#########

# Background
bg_color white
set ray_opaque_background, 0

# Lighting
set ambient, 0.2
set ray_shadows, 1
set spec_reflect, 0.6
set spec_power, 600
set spec_count, 3
```

```
set shininess, 70
set reflect, 0.5

# General visuals
set ray_trace_mode, 1
set ray_texture, 2
set antialias, 3
set fog, 1
set fog_start, 0.4

# Orientation
# insert what you get from pressing "Get View" in PyMol to save
# current molecule orientation

#set_view (<XYZ>)

# save
#png <molecule_MEP>.png, width=1600, height=1200, dpi=300, ray=1
#quit
```

The spin density was visualized with the following PyMOL script:

```
load NAME.xyz,
mol load NAME.spindens.cube, sd

##########
# molecule
##########

show sticks, mol
hide lines, mol
set_bond stick_radius, 0.1, mol

# colors
color gray70, (elem C)
color white, (elem H)

#########
# spin
#########
isosurface spin_pos, sd, 0.005
isosurface spin_neg, sd, -0.005

# colors
color blue, spin_pos
color red, spin_neg

#########
# general
#########
```

```
# Background
bg_color white
set ray_opaque_background, 0

# Lighting
set ambient, 0.2
set ray_shadows, 1
set spec_reflect, 0.6
set spec_power, 600
set spec_count, 3
set shininess, 70
set reflect, 0.5

# General visuals
set ray_trace_mode, 1
set ray_texture, 2
set antialias, 3
set fog, 1
set fog_start, 0.4


# save
#png <molecule_MEP>.png, width=1600, height=1200, dpi=300, ray=1
#quit
```

Frontier Molecular Orbitals

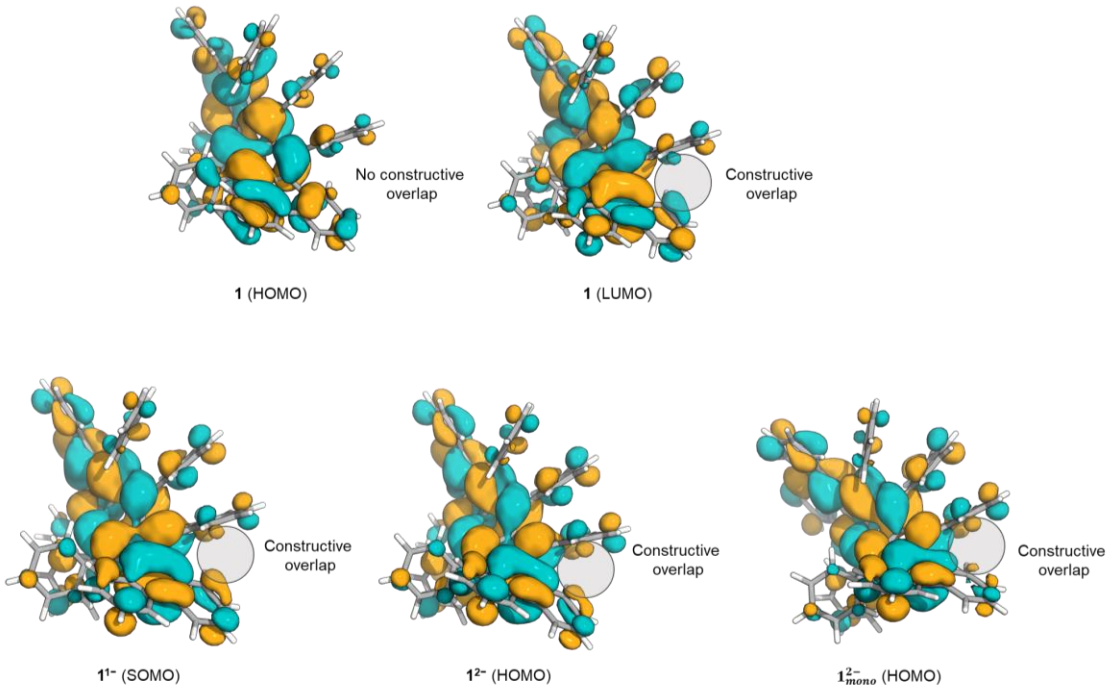

Figure S18. Frontier molecular orbitals for $\mathbf{1}$, $\mathbf{1^{1-}}$, $\mathbf{1^{2-}}$, and $\mathbf{1^{2-}_{mono}}$. Constructive overlaps that promote cyclization are highlighted. The orbitals are plotted at the isosurface value α = 0.15 a.u.

Electrostatic Potential Maps

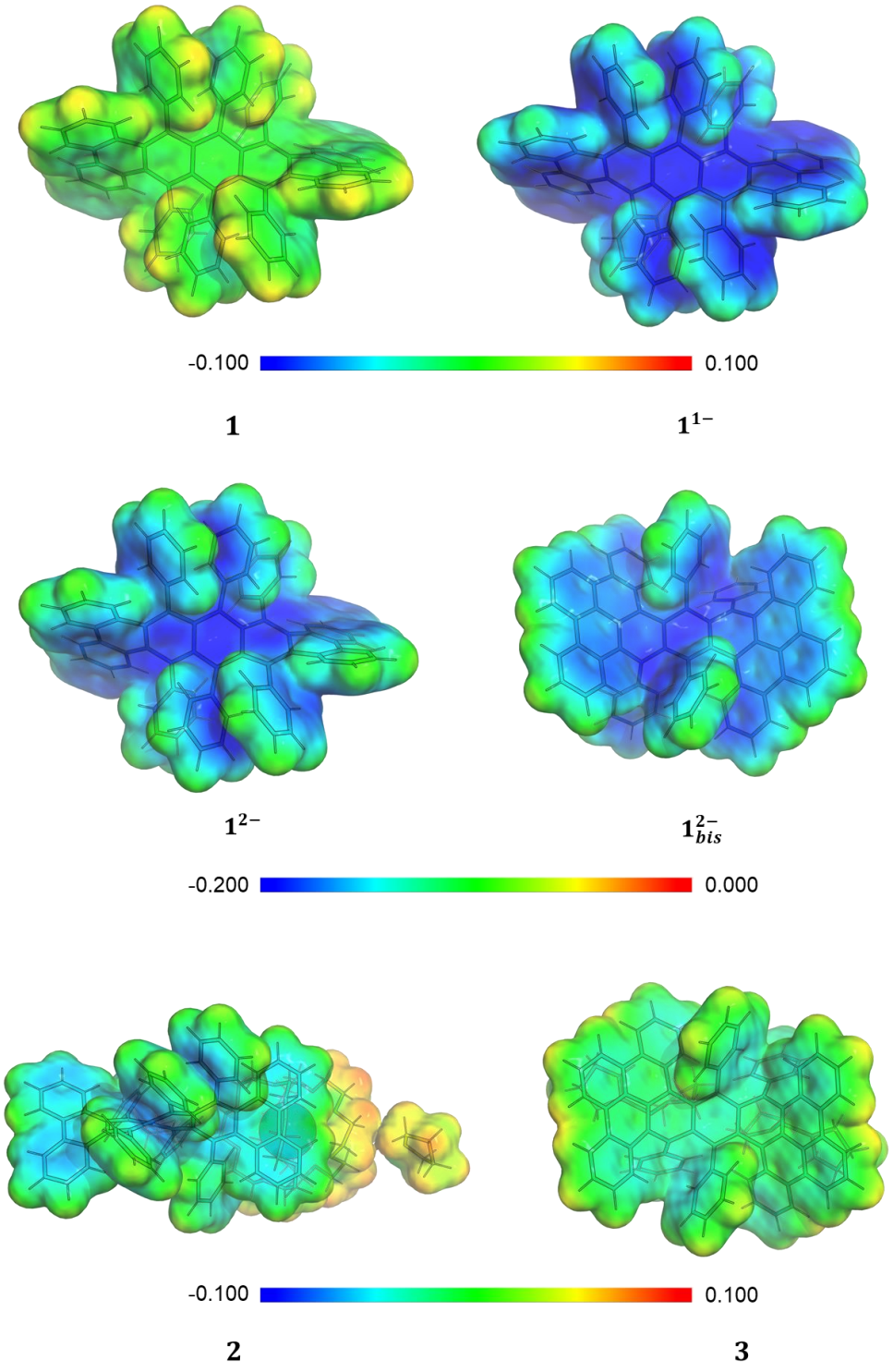

Figure S19. Electrostatic potential maps for **1**, $\mathbf{1^{1-}}$, $\mathbf{1^{2-}}$, $\mathbf{1^{2-}_{bis}}$ and complexes **2** and **3** (the metal moiety is omitted for clarity).

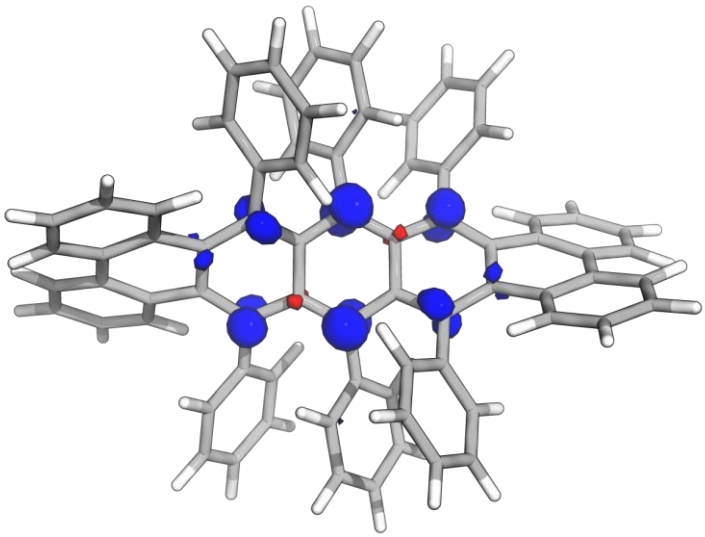

Figure S20. Total spin density plot for $\mathbf{1}^{\mathbf{1-}}$. Positive spin density is shown in blue, and negative spin density is shown in red.

VII. References

1 N. V. Kozhemyakina, J. Nuss and M. Jansen, *Z. Für Anorg. Allg. Chem.*, 2009, **635**, 1355–1361.
2 J. Lu, D. M. Ho, N. J. Vogelaar, C. M. Kraml, and R. A. Pascal, *J. Am. Chem. Soc.*, 2004, **126**, 11168–11169.
3 SAINT; part of Bruker APEX3 software package (version 2017.3-0): Bruker AXS, 2017.
4 SADABS; part of Bruker APEX3 software package (version 2017.3-0): Bruker AXS, 2017.
5 G. M. Sheldrick, *Acta Crystallogr.*, 2015, **A71**, 3–8.
6 G. M. Sheldrick, *Acta Crystallogr.*, 2015, **C71**, 3–8.
7 O. V. Dolomanov, L. J. Bourhis, R. J. Gildea, J. A. K. Howard and H. Puschmann, *J. Appl. Crystallogr.*, 2009, **42**, 339–341.
8 F. Neese, F. Wennmohs, U. Becker and C. Riplinger, *J. Chem. Phys.*, 2020, **152**, 224108.
9 J. P. Perdew, K. Burke and M. Ernzerhof, *Phys. Rev. Lett.*, 1996, **77**, 3865–3868.
10 C. Adamo and V. Barone, *J. Chem. Phys.*, 1999, **110**, 6158–6170.
11 F. Weigend and R. Ahlrichs, *Phys. Chem. Chem. Phys.*, 2005, **7**, 3297.
12 D. Rappoport and F. Furche, *J. Chem. Phys.*, 2010, **133**, 134105.
13 S. Grimme, J. Antony, S. Ehrlich and H. Krieg, *J. Chem. Phys.*, 2010, **132**, 154104.
14 S. Grimme, S. Ehrlich and L. Goerigk, *J. Comput. Chem.*, 2011, **32**, 1456–1465.
15 P. v R. Schleyer, C. Maerker, A. Dransfeld, H. Jiao and N. J. R. van Eikema Hommes, *J. Am. Chem. Soc.*, 1996, **118**, 6317–6318.
16 R. Gershoni-Poranne and A. Stanger, in *Aromaticity*, Ed. I. Fernandez, Elsevier, 2021, 99–154.
17 A. P. Rahalkar and A. Stranger, *Aroma*, 2014.
18 T. Lu and F. Chen, *J. Comput. Chem.*, 2012, **33**, 580–592.
19 T. Lu and F. Chen, *J. Mol. Graph. Model.*, 2012, **38**, 314–323.
20 *The PyMOL Molecular Graphics System*, Schrödinger, LLC: 2014.
21 R. Gershoni-Poranne and A. Stanger, *Chem. – Eur. J.*, 2014, **20**, 5673–5688.